WATER RESOURCES RESEARCH, VOL. 36, NO. 12, PAGES 3743–3755, DECEMBER 2000

# Variability of bed mobility in natural, gravel-bed channels and adjustments to sediment load at local and reach scales

Thomas E. Lisle,[1] Jonathan M. Nelson,[2] John Pitlick,[3]
Mary Ann Madej,[4] and Brent L. Barkett[3]

**Abstract.** Local variations in boundary shear stress acting on bed-surface particles control patterns of bed load transport and channel evolution during varying stream discharges. At the reach scale a channel adjusts to imposed water and sediment supply through mutual interactions among channel form, local grain size, and local flow dynamics that govern bed mobility. In order to explore these adjustments, we used a numerical flow model to examine relations between model-predicted local boundary shear stress ($\tau_j$) and measured surface particle size ($D_{50}$) at bank-full discharge in six gravel-bed, alternate-bar channels with widely differing annual sediment yields. Values of $\tau_j$ and $D_{50}$ were poorly correlated such that small areas conveyed large proportions of the total bed load, especially in sediment-poor channels with low mobility. Sediment-rich channels had greater areas of full mobility; sediment-poor channels had greater areas of partial mobility; and both types had significant areas that were essentially immobile. Two reach-mean mobility parameters (Shields stress and $Q^*$) correlated reasonably well with sediment supply. Values which can be practicably obtained from carefully measured mean hydraulic variables and particle size would provide first-order assessments of bed mobility that would broadly distinguish the channels in this study according to their sediment yield and bed mobility.

## 1. Introduction

Channel evolution is a response to runoff and sediment supply involving mutual interactions among channel form, bed material size, and hydraulic forces. In the short term these interactions are driven by spatial variations in boundary shear stress acting on bed material of varying mobility. In most gravel-bed channels, mean boundary shear stress only slightly exceeds the threshold for particle entrainment at channel-forming (bank-full) flows [*Parker*, 1979; *Andrews*, 1983]. Such channels are commonly referred to as "threshold channels."

A question that we address is, How well are boundary shear stress and bed-surface particle size adjusted within a reach of a threshold channel? Four degrees of adjustment could govern channel evolution: (1) Variations in bed-surface particle size are balanced by variations in boundary shear stress so that threshold conditions are met uniformly over the channel. Conditions are constrained near threshold in order to maintain an active bed with weak bed load transport, which is characteristic of gravel-bed channels. Uniform threshold conditions are the basis for the design of stable artificial channels [*Lane*, 1955]. (2) Variations in local shear stress and surface particle size create zones of higher or lower transport, but stability in channel form is maintained throughout the range of sediment-transporting flows because divergence in local boundary shear stress is balanced by local sediment transport rate and particle size; thus local transport capacity is fulfilled everywhere by local sediment supply [*Dietrich and Whiting*, 1989]. (3) Imbalances in local transport capacity and supply occur as stage rises and falls, but the channel returns to the same form and texture after each flood hydrograph. Such a pattern has been observed in detailed measurements of flow and sediment transport in sand- and gravel-bedded channels [*Dietrich and Whiting*, 1989; *Ferguson et al*., 1989] and in stage-dependent scour and fill of riffles and pools [*Keller*, 1971; *Andrews*, 1979; *Sear*, 1996]. (4) Secular variations in local shear stress, surface particle size, and sediment supply cause the channel to deform and migrate across the valley bottom while maintaining the same basic form. Degree 1 contrasts with degrees 2–4, which are not mutually exclusive. Instead, each degree from 2 to 4 becomes more valid successively at larger timescales. These issues can be elucidated by examining patterns of local boundary shear stress and surface particle size.

Flume experiments have indicated that the heterogeneity of particle sizes in gravel-bed channels provides a capacity for adjusting to changes in sediment load through changes in the mobility of the bed surface. *Dietrich et al*. [1989] fed mixed-size sediment at a high rate into a narrow flume containing bed material with the same size mixture as the feed and then reduced the feed rate in two steps after achieving equilibrium in sediment transport during each step as boundary shear stress was held approximately constant. At the initial, highest feed rate a coarse surface layer was not evident. After each subsequent reduction in feed rate the surface coarsened over most of the bed. In total, a 90% reduction in feed rate resulted in a 32% increase in median surface particle size ($D_{50}$). Despite nearly uniform hydraulic conditions a relatively fine zone was maintained where most of the bed load was transported. *Lisle et al*. [1993] observed similar but stronger textural adjustments in a wider experimental channel with alternate bars. A

[1]Pacific Southwest Research Station, U.S. Forest Service, Arcata, California.
[2]U.S. Geological Survey, Denver, Colorado.
[3]Department of Geography, University of Colorado, Boulder.
[4]U.S. Geological Survey, Arcata, California.



Paper number 2000WR900238.
0043-1397/00/2000WR900238$09.00

90% reduction in feed rate resulted in a 62% increase in $D_{50}$ averaged over the patchy bed surface.

The results of these experiments are the basis for the hypothesis that an increase in the quantity of sediment entering a natural gravel-bed channel (disregarding changes in sediment caliber) causes the bed surface to become finer, thus offering less resistance to tractive forces [*Dietrich et al*., 1989]. Higher equilibrium bed load transport rates can be achieved without requiring channel morphology alone to respond. *Dietrich et al*. [1989] quantify this adjustment with $q^*$, the ratio of bed load transport predicted from bed-surface particle size to that predicted from the particle size of the load. As armoring increases, the bed load transport rate predicted from surface material becomes a smaller fraction of that predicted from bed load material. Here $q^*$ can be regarded as a measure of transport efficiency: A value of $q^* = 1$ signifies that the supply of bed load is so high that armoring no longer exists, and further increases in supply must be accommodated by aggradation; a value of $q^* = 0$ signifies a cessation of transport. The validity of the hypothesis is supported by a new analysis by *Buffington and Montgomery* [1999] of previous experimental results that involves a more precise partitioning of boundary shear stress acting on bed particles.

Application of the experimental results to natural channels remains uncertain because transport rates and particle sizes in the experiments were imposed by sediment feed. In contrast, bed load transport in natural channels is more or less dependent on sediment supply, depending on the scale of time and space over which it is observed [*Wilcock and Southard*, 1989]. Under intensive bed load transport the bed surface becomes finer as particles that represent the size distribution of the load, which is finer than the winnowed surface layer, begin to inundate the bed surface [*Parker and Klingeman*, 1982]. This results in a smoother bed that is more mobile for all sizes. Intensive transport rates can be associated with either high sediment supply or high boundary shear stress in excess of particle entrainment. These causes are inseparable to some degree because excess shear stress and particle size mutually adjust to both flow intensity and sediment supply [*Buffington and Montgomery*, 1999]. In either case, intensive transport must be supported by high supply; otherwise, the bed winnows and coarsens. *Kinerson* [1990] and we attempt to sort out stage-dependent variations in shear stress by using a reference stage (bank-full) to measure hydraulic variables.

Steady flow conditions were also imposed in the experiments in order to achieve equilibrium in sediment transport; thus surface particle sizes were not affected by hydrographs, as would occur in natural channels. A critical issue is whether bed-surface composition at bank-full stage in natural channels is preserved for low stages when the bed can be easily measured. *Andrews and Erman* [1986] found no difference between bed-surface particle size measured at a flood stage and at a low stage in Sagehen Creek, but a low sediment supply may have inhibited the intensity of bed load transport and stage-dependent surface fining. Selective transport during waning stages of a bank-full event may winnow parts of the bed surface of fine material but enrich the bed with fines elsewhere as a result of locally diverging hydraulic conditions [*Lisle and Hilton*, 1999]. Stage-dependent changes in bed texture are important in understanding the dynamics of natural gravel-bed channels.

The hypothesis of the adjustment of bed mobility to sediment supply remains to be fully tested and adapted to natural channels. *Kinerson* [1990] measured values of $q^*$ based on reach-averaged, bank-full boundary shear stress and surface and subsurface bed material size in eight natural channels and found a correlation between $q^*$ and evaluations of sediment supply. Decreases in mean boundary shear stress and increases in bed-surface particle size were associated with declining supplies of sediment in the Toutle River, Washington, following the 1980–1983 eruptions of Mount St. Helens [*Simon and Thorne*, 1996].

In this paper we examine the balance between local boundary shear stress and bed-surface particle size in six natural gravel-bed channels with alternate bars at the local scale (areas of $10^0$ m$^2$) and reach scale (several channel widths or more long). We chose this type of channel to represent common, self-formed, threshold channels that are moderately stable. At the local scale we used a three-dimensional flow model to compare the spatial distribution of model-generated boundary shear stress at bank-full stage with surface particle size measured in the field. These variables were poorly correlated, which may account for stage-dependent and secular evolution of channel form. Predicted values of local bed load transport rate indicate that areas of high transport convey a large majority of the total load. At the reach scale we examined how a wide range in sediment supply can affect bed mobility, as quantified by two reach-averaged parameters: Shields stress and $Q^*$ (the uppercase indicating a reach-averaged value of $q^*$). Our purpose is to test if practicably measured mobility parameters can be used to evaluate textural adjustments to sediment supply in natural channels.

## 2. Study Reaches

We examined six channels in northwestern California and western Colorado (Table 1). The California study reaches are within 40 km of the Pacific coast; the Colorado channels are tributaries of the upper Colorado River. The Redwood Creek study reaches are described by *Lisle and Madej* [1992]; Jacoby Creek is described by *Lisle* [1986, 1989]; and Gunnison River and Williams Fork study reaches are described by *Barkett* [1998]. All study reaches are self-formed, slightly sinuous gravel channels with one to five alternate bars, but they differ in size and sediment supply. Channels are composed predominantly of gravel with varying fractions of sand. Bed surfaces are weakly to strongly armored (Figure 1), but the full range of bed particle sizes are transportable during flood stages. Study reaches were 3 to 22 channel widths long.

The California channels have high sediment yields resulting from high uplift rates, erodible bedrock, high variability in runoff rates, and recent disturbance from logging and road building. As a result, the channels are periodically very active. Rates of sediment yield of Redwood Creek and Grouse Creek are among the highest in the coterminous United States. The basins of the California channels are unglaciated. Valleys are steep and narrow and consist mostly of sandstones, shales, and low-grade metamorphic rocks with thin mantles of alluvium and colluvium. Peak discharges result from rainfall and rain on snow. The two study reaches of Redwood Creek are separated by 12 river km.

The Colorado rivers have a much lower sediment yield, but the channels are active. The Gunnison River study reach is located in a broad valley underlain by sandstone and shale formations covered by alluvium and colluvium. The Williams Fork study reach is located in a glaciated valley underlain by metamorphic and intrusive igneous bedrock overlain by thin

**Table 1.** Characteristics of Study Reaches

| Reach (Location) | Drainage Area, km$^2$ | Sediment Yield,[a] Mg km$^{-2}$ yr$^{-1}$ | Bank-full Discharge, m$^3$ s$^{-1}$ | Channel Gradient | Bank-full Width, m | Reach Length, m | $\overline{D_{50}}/\overline{D_{s50}}$[b], mm |
|---|---|---|---|---|---|---|---|
| Redwood Creek 1, California (41°16′N, 124°01′E) | 600 | 1400 | 430 | 0.0018 | 100 | 1800 | 11/6.3 |
| Redwood Creek 2, California (41°12′N, 124°0′E) | 520 | 1400 | 370 | 0.0026 | 60 | 1300 | 15/11 |
| Grouse Creek, California (40°43′N, 123°34′E) | 140 | 1800 | 93 | 0.0064 | 33 | 315 | 39/13 |
| Jacoby Creek, California (40°50′N, 124°02′E) | 36 | 180 | 14 | 0.0060 | 12 | 198 | 36/13 |
| Gunnison River, Colorado (38°44′N, 108°9′E) | 9600 | 75 | 325 | 0.0012 | 101 | 280 | 35/19 |
| Williams Fork, Colorado (39°50′N, 106°4′E) | 231 | 0.1 | 11 | 0.0049 | 25 | 138 | 32/27 |

[a]Mean annual basin yields for clastic sediments are given. Locations and sources are as follows: Redwood Creek (M. A. Madej, unpublished data, 1998), Grouse Creek [*Raines and Kelsey*, 1991], Jacoby Creek [*Lehre and Carver*, 1985], Gunnison River [*Van Steeter and Pitlick*, 1998], and Williams Fork [*Andrews and Nankervis*, 1995].

[b]$\overline{D_{50}}$ and $\overline{D_{s50}}$ are reach-averaged median particle sizes of the bed surface and subsurface, respectively. Their ratio represents the degree of armoring.

veneers of till or colluvium. Flow regimes of both Colorado rivers are dominated by snowmelt peaks, but Gunnison River flow is affected by upstream dams and diversions.

## 3. Methods

### 3.1. Data Collection

We mapped channel topography and bed material size at low flow when the channels were accessible. In the California channels we mapped bed-surface material as three to five patch types. Patches are bed areas of quasi-uniform surface material that are delineated in areas of $10^0$–$10^2$ m$^2$ and tend to be larger in larger channels. Patch types represent common particle-size ranges observed in each channel (Table 2). We delineated patch boundaries by visually estimating where $D_{75}$ (particle size for which 75% by weight are finer) of the surface particles better represented one or another patch type. We did pebble counts ($n \geq 100$ [*Wolman*, 1954]) on randomly selected patches from each type, so that counted patches had specific particle sizes, and the remainder were given mean sizes for their patch type. We also sampled subsurface material from randomly selected patches by removing the surface layer to a depth roughly equal to the largest surface particles and obtaining a subsurface sample about twice as thick. Sampling methods used in the California channels and particle sizes for the Redwood Creek reaches are reported elsewhere [*Lisle and Madej*, 1992].

We did not map patches in the Colorado channels. Instead, we measured local variations in surface particle size with pebble counts ($n \geq 100$) in 4-m$^2$ areas that were spaced 20 m apart along Gunnison River cross sections (a total of 36 counts) and 5 m apart along Williams Fork cross sections (48 counts). Cross sections were spaced every 25 m in Gunnison River and every 10 m in Williams Fork. We sampled subsurface bed material from channel bars in a similar manner as in the California channels; averages of three samples from Gunnison River and two from Williams Fork represent each reach as a whole.

### 3.2. Flow Model

Model predictions of boundary shear stress patterns at bankfull flow were obtained from a quasi-three-dimensional flow model. The model comprises two components: a solution of the full vertically averaged and Reynolds-averaged momentum

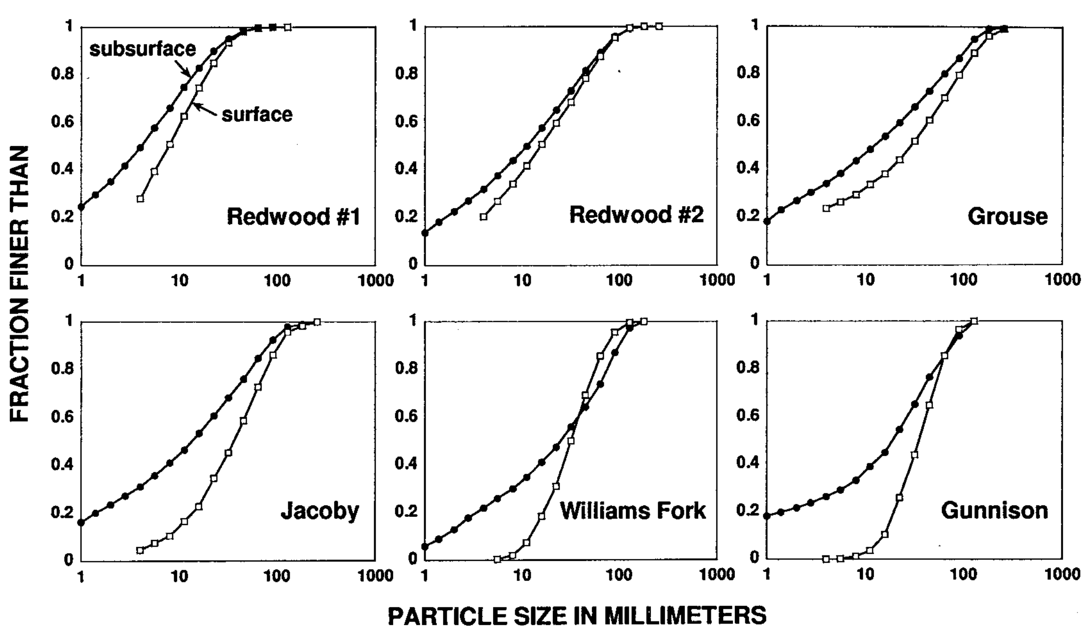


**Figure 1.** Area-weighted average surface and subsurface particle size distributions.

**Table 2.** Area and Particle Size Statistics of Patch Types

| Patch Type | Bed Area, % | $n$ | Mean $D_{50}$,[a] mm | Mean $\sigma_\phi$ |
|---|---|---|---|---|
| Redwood 1 | | | | |
| Fine pebble | 23.8 | 16 | 6.1 (1.5) | 1.6 |
| Coarse pebble | 56.6 | 19 | 14.9 (3.5) | 1.5 |
| Cobble | 19.6 | 15 | 30.0 (5.4) | 1.4 |
| Redwood 2 | | | | |
| Fine pebble | 27.5 | 6 | 5.0 (1.2) | 1.4 |
| Coarse pebble | 43.4 | 13 | 23.5 (4.9) | 1.7 |
| Cobble | 19.8 | 8 | 38.8 (8.2) | 1.8 |
| Bimodal | 9.3 | 5 | 11.0 (9.3) | 2.5 |
| Grouse Creek | | | | |
| Fine pebble | 16.7 | 5 | 1.5 | 1.6 |
| Coarse pebble | 31.1 | 5 | 28.1 (6.2) | 1.8 |
| Cobble | 34.1 | 5 | 83.0 (16.3) | 1.6 |
| Bimodal | 18.1 | 5 | 11.3 (11.9) | 2.7 |
| Jacoby Creek | | | | |
| Fine pebble | 8.5 | 2 | 2.2–7.8 | 1.4 |
| Coarse pebble | 38.9 | 2 | 26.7–26.8 | 1.4 |
| Cobble | 52.7 | 2 | 36.4–49.6 | 1.3 |

[a]Standard deviation is given in parentheses.

equations and a vertical-structure submodel that determines the distribution of velocity in the vertical along the streamlines of the vertically averaged flow and the secondary flows across the streamlines of the vertically averaged flow. The full vertically averaged equations used in the computational solution are cast in a channel-fitted curvilinear coordinate system; these equations are given by *Nelson and Smith* [1989, equations (8) and (9)]. The vertically averaged part of the model computes fields of surface elevation and downstream and cross-stream components of both vertically averaged velocity and bottom stress. Inputs to the vertically averaged model are discharge, topography, and roughness (either in the form of roughness lengths or drag coefficients). The vertical-structure part of the model yields downstream and cross-stream components of velocity and Reynolds shear stress at discrete points in the vertical and also yields the structure of secondary flows and modifications to the bed stress associated with secondary flows. Inputs to the vertical-structure component of the model are eddy viscosity structure functions and the results of the vertically averaged model. The approach uses the assumptions that (1) the flow is steady (or at least does not vary appreciably over short timescales), (2) the flow is hydrostatic (vertical accelerations are neglected), and (3) the turbulence can be treated adequately by relating Reynolds stresses to shears using an isotropic eddy viscosity.

The numerical solution solves the full vertically averaged equations using a combination of an explicit solution of the momentum equations with an implicit solution for updating surface elevations. The explicit technique incorporates operator splitting and upwind differencing to enhance stability and convergence characteristics of the approach, especially in regions where flow separation occurs. The surface elevation is calculated using the semi-implicit method for linked equations (SIMPLE) [*Patankar*, 1980], which comprises an alternating-direction implicit scheme with operator splitting and a tridiagonal matrix solver. Elevation and velocity fields are updated at each iteration of the model using differential relaxation, and iteration continues until both mass and momentum conservation are satisfied to an extremely high degree of accuracy at every point in the computational grid.

Using the solutions from the vertically averaged model, an assumed eddy viscosity structure from *Rattray and Mitsuda* [1974], and a spatial distribution of roughness lengths or drag coefficients, the vertical-structure component of the model yields a full three-dimensional flow solution. Boundary conditions for the model runs were given as velocity at the upstream end of the grid and surface elevation at the downstream end of the grid.

For the model runs used in this paper, the hydraulic roughness was calibrated using observed water surface profiles. There are two possible ways to do this. One could assume that the flow averages the roughness over the reach and that drag coefficients should be spatially constant. However, one could assume that flow responds instantaneously to local grain size, and hydraulic roughness in a mixed grain system should be set locally using local grain size. In reality, bottom stress and turbulence structure adjust spatially to a change in roughness along the flow streamlines in a complicated manner [*Antonia and Luxton*, 1971, 1972]. Explicitly accounting for this adjustment would require using a turbulence closure that treated advection of the turbulence field (e.g., a $k$-$\varepsilon$ or full Reynolds equations model). However, the two methods described above are equivalent to assuming that the flow responds extremely slowly to changes in roughness (constant drag coefficient) or that it responds essentially instantaneously to changes in roughness (local drag is related directly to local grain size). Obviously, the truth is somewhere in between these two extremes, so model runs were done both ways to examine the sensitivity of the results to the roughness distribution. First, model runs were completed by using a constant drag coefficient (equivalent to assuming that local roughness lengths are proportional to depth) and setting the value of that coefficient such that the predicted surface elevation drop through each reach matched the observed value. In a second set of runs, local roughness length was assumed to be proportional to local bed grain size, meaning that the local drag coefficient was approximately logarithmically dependent on local grain size. Using this spatial dependence, a constant multiple (a single number for the entire reach) was adjusted to produce the observed elevation drop. Both methods gave reasonable results, with the first method producing drag coefficients in the range of 0.003 to 0.01, with most reaches clustered in the middle of this range, as expected. The method using the local bed grain size gave surprisingly similar results for the bottom stress field. This occurs because the effect of including grain size in the drag distribution was to make coarser areas rougher and fine areas smoother, tending to decrease velocities over rough areas and increase them over smoother areas. Thus, over the coarse areas, the drag coefficient was higher, but the velocity was slightly lower, and over the finer areas the opposite was true. Since local stress is primarily dependent on the drag coefficient times the velocity squared, the net effect on the stress was smaller than the effect on either the velocity or the drag coefficient. This is largely true because the drag coefficient only depends on grain size logarithmically, and for typical ranges of grain sizes in the streams of interest the range in the drag coefficient was not very high. In any case, the conclusions presented here appear to be independent of which roughness model is used, which is a particularly advantageous result.

For the cases presented herein, form drag due to bars and bed forms in these predominantly gravel-bed reaches was assumed to be negligible relative to grain drag, so computed bottom stresses were used directly for local bed stress. However, it is important to note that even if form drag due to bars and bed forms were present, spatial correlations between grain size and bottom stress would be unchanged, as that form drag is typically removed uniformly over the reach. However, if the methodology were employed to investigate situations with great variability in the occurrence or geometry of bars and bed forms within the reach, then the spatial variation of form drag within the reach should be explicitly accounted for. For the study reaches, bed slopes along flow streamlines were typically small, and bed forms were typically not present, so it was appropriate to assume grain drag was dominant.

To examine the accuracy of the model for routing the flow through the reaches, predicted vertically averaged velocities were compared to measured values at the Redwood 2 reach (Figure 2). The agreement is reasonably good and is similar to the accuracy of other two- and three-dimensional flow predictions for channels of this type. Given that the routing of the flow was reasonably well predicted and that the total drag on the channel was accounted for by ensuring that the total head loss was correctly predicted, the predicted values of boundary shear stress should provide good estimates of the actual values, especially in these systems, which are dominated by grain roughness.

We computed predicted values of local bed load transport rate at bank-full stage from local values of boundary shear stress and surface particle size by using *Parker*'s [1990] surface-based bed load function for gravel-bed channels. We chose the Parker function because it is based on particle sizes of the bed surface and explicitly incorporates the variation of transport rates with Shields stress in the range of marginal transport, which was prevalent in our channels. Shields stress ($\tau_j^* = \tau_j/RD_{50j}$, where $\tau_j$ is local boundary shear stress, $R$ is submerged specific gravity of sediment, and $D_{50j}$ is local median particle size of the bed surface) is a commonly used mobility parameter that represents the ratio of tractive and gravitational forces acting on bed particles. The Parker function predicts transport rates of individual size fractions of substrate material by predicting the evolution of surface particle size distribution from the subsurface distribution as transport intensifies. It is theoretically founded on the behavior of active armor layers, but the governing equations are empirically derived from data from Oak Creek, Oregon, and linearly scaled for adapting to other channels. We used our data to examine variations in relative rates of bed load transport within and between channels. In order to do so, we made some simplifying assumptions and computed the transport rate only for the median particle size of the reach-averaged subsurface material ($\overline{D_{s50}}$). We did not scale the transport rate of the median size range by its fraction on the bed surface. A dimensionless transport rate was adapted from *Parker* [1990],

$$W_{s50}^* = Rgq_{s50}/(\tau_j/\rho)^{3/2}, \tag{1}$$

(where $g$ is gravitational acceleration, $q_{s50}$ is the volumetric transport rate per unit width of the reach-averaged median subsurface particle size ($\overline{D_{s50}}$), and $\rho$ is fluid density). We computed $W_{s50}^*$ from an adaptation of (28) of *Parker* [1990]:

$$W_{si}^* = 0.00218G[\omega\phi_{sg0}g_0(\partial_i)], \tag{2}$$

where $G$ is a function of the values in brackets.

The "straining function" $\omega$ varies with the degree of armoring: It equals approximately 1 during low transport stages when armoring is most highly developed and decreases at higher transport stages as armoring diminishes. We measured $D_{50j}$ at low stages and assumed that $\omega = 1$ everywhere at bank-full stage. This simplifying assumption is justified by the fact that most areas of the bed achieving high transport stages ($\tau_j^* > 0.06$) at bank-full were already poorly armored and thus not likely to undergo significant changes in $D_{50j}$ because of increasing transport intensity, while well-armored areas generally did not achieve high Shields stresses.

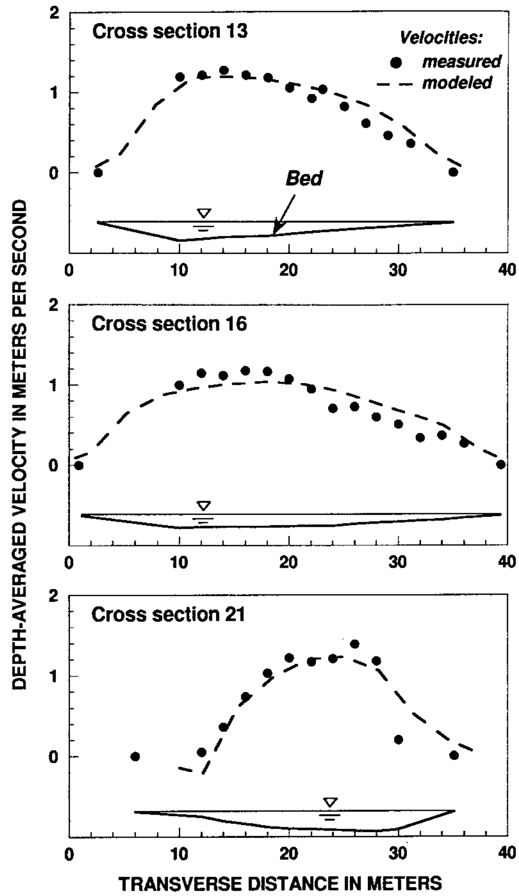


**Figure 2.** Comparison of model-generated, vertically averaged flow velocity and mean vertical velocity represented by measurements at 0.6 times depth from the water surface in three cross sections of Redwood Creek 2 at a discharge of 25 $m^3\ s^{-1}$.

The variable $\phi_{sg0}$ is Shields stress scaled by a reference Shields stress of 0.0386. In Parker's formulation, Shields stress ($\tau_{sg}^*$) is calculated from the geometric mean surface particle size ($D_{sg}$), which we found to be satisfactorily approximated by $D_{50j}$ in our channels. We applied the former assumption of constant $D_{50j}$ with changing stage and substituted $\tau_j^*$ for $\tau_{sg}^*$.

Finally, $g_0$ is a hiding function that adjusts the mobility of a particle size relative to the surface size distribution and is evaluated by $g_0 = (D_i/D_{sg})^{-\beta}$, where $\beta = 0.0951$. The value of $\beta$ was adopted from Oak Creek, a well-armored channel. This introduced error of unknown magnitude because $\beta$ can vary between channels [*Ashworth and Ferguson*, 1989; *Parker*, 1990], but we do not believe it significantly affected our results. Using the previous substitutions, $g_0 = (\overline{D_{s50}}/D_{50j})^{-\beta}$.

## 4. Patterns of Local Boundary Shear Stress and Surface Particle Size

We use Redwood Creek 1 at bank-full stage as an example to show spatial patterns of topography, flow, boundary shear

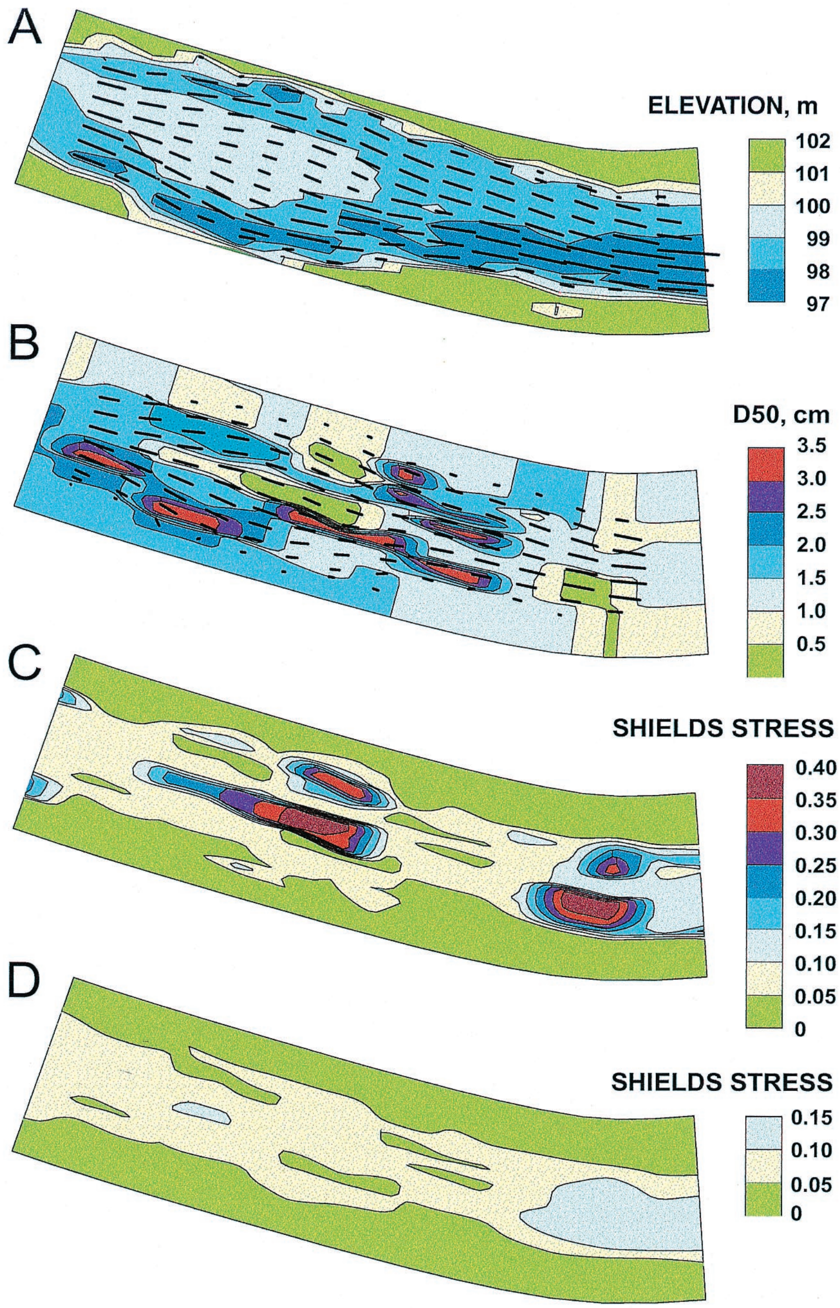


**Plate 1.** Model outputs of an upstream section of the Redwood Creek study reach 1. (a) Bed topography and unit-discharge vectors. (b) Bed surface particle size and boundary shear stress vectors. (c) Shields stress computed from measured $D_{50}$. (d) Shields stress computed with fine material stripped from the bed surface. For clarity, one half of the vectors have been removed. Blocky patterns of $D_{50}$ at channel margins (Plate 1b) should be ignored. They represent values of $D_{50}$ that were projected outside of the active channel and were not included in the analysis.

stress, and surface particle size that were common to all channels, although particle sizes in the Colorado channels were not as variable. Bed topography and unit-discharge vectors (Plate 1a) displayed patterns that are common in channels with alternate bars. Flow alternately diverged and decelerated over shoaling bar surfaces and converged and accelerated into troughs.

Patterns of boundary shear stress were inconsistent with those of surface particle size (Plate 1b). On one hand, shear stress was characteristically low over fine-grained, distal bar surfaces and inner bar margins and was high over coarse patches on bar heads. On the other hand, shear stress was also low over some coarse channel margins and high in fine-textured troughs. These differences are better revealed by patterns of $\tau_j^*$ (Plate 1c), which showed considerable variation. In particular, zones of extremely high $\tau_j^*$ appeared in fine-grained areas such as troughs. The apparent lack of correlation was confirmed by regressing local boundary shear stress against bed-surface particle size ($r = 0.27$, Figure 3a).

Troughs characteristically contained some of the largest patches of fine bed material (Figure 4). We believe that as flow decreases, fine bed load (sand and fine gravel) is selectively transported from stabilizing armor layers and deposited as fine patches in zones of low or downstream-decreasing shear stress that are commonly located in troughs or pools. During floods, high stresses resulting in suspension and intensive bed load transport of fine material can scour these patches and expose an underlying coarser bed [*Lisle and Hilton*, 1999]. Stage-dependent sorting mechanisms such as this indicate that bed-surface particle sizes measured at low flow may not everywhere represent those at high flow.

In order to more accurately represent surface particle size during high flow, we computationally "stripped" highly mobile fine areas by employing a simple rule: At points where $\tau_j^* > 0.1$ and particle size is that of a fine patch, assign the particle size of the adjacent coarser patch to the point and recalculate $\tau_j^*$. This was not done for the Colorado reaches, which did not have extensive fine patches. This forced a better correlation between boundary shear stress and surface particle size (Figure 3b, $r = 0.41$), but our aim is not to rationalize a better correlation but to more accurately represent bed material size distributions at high flow.

In fact, one of our main conclusions from this study is that boundary shear stress and bed-surface size were essentially uncorrelated. Absolute values of $r$ for the other channels were less than that for Redwood 1, and all but Redwood 1 and Gunnison had negative values of $r$ at bank-full stage.

Stripping of fines from zones of extreme $\tau_j^*$ created a smoother pattern (Plate 1d). Nevertheless, adjusted $\tau_j^*$ still displayed substantial variation, indicating that threshold conditions were not uniformly met over the channel. There were large-scale variations in $\tau_j^*$ longitudinally as well as transversely, indicating streamwise discontinuities in bed load transport. The implications of this will be discussed in section 7.1.

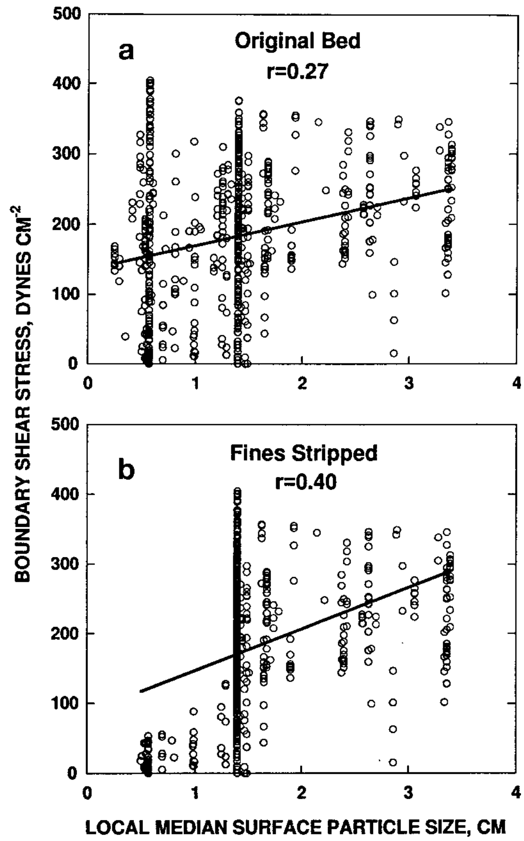


**Figure 3.** Local boundary shear stress versus local median surface particle size in Redwood Creek Reach 1 at bank-full stage (a) for original bed material and (b) with fine material computationally stripped.

## 5. Frequency Distributions

We used frequency distributions to compare the variability of parameters related to the mobility of the six channels without regard to specific topographic features.

### 5.1. Boundary Shear Stress

Frequency distributions of local boundary shear stress normalized by the median value for the reach ($\tau_j/\tau_{50}$) were similar (Figure 5a). Peak frequencies fell around $\tau_j/\tau_{50} = 1$, and tails of the distributions extended beyond $\tau_j/\tau_{50} = 2$. Grouse and Jacoby Creeks showed the broadest distributions, perhaps because as the smallest channels, they are likely to be most affected by form roughnesses such as woody debris and bank protrusions that are large relative to channel size.

### 5.2. Shields Stress

To compare frequency distributions of $\tau_j^*$, we used three reference values of $\tau^*$ that differentiate the intensity and size selectivity of bed load transport: We assumed that beds are stable below an entrainment threshold of $\tau_c^* = 0.03$. We assumed that partial transport, where some particles of a given size on the bed surface are active while others of the same size are immobile, occurs for $\tau_c < \tau < 2\tau_c$, where $\tau_c$ corresponds to the entrainment threshold [*Wilcock and McArdell*, 1997]. Thus partial transport corresponds to $0.03 < \tau^* < 0.06$. We assumed that particles larger than $D_{50}$ are equally mobile and that $\tau^* > 0.06$ (computed from $D_{50j}$) approximates fully mobile bed conditions. Values of $\tau^* > 0.15$ indicate intensive bed load transport that could be expected to occur only locally or during extreme floods in gravel-bed channels. These values occurred only in Redwood and Grouse Creeks.

Frequency distributions of bankfull $\tau_j^*$ showed strong differences between the six channels (Figure 5b). Using reference values of $\tau^*$, we classified our channels as "partially mobile" or "fully mobile." In partially mobile channels (Jacoby Creek, Gunnison River, and Williams Fork), values of $\tau_j^*$ were mostly less than 0.06, and values in the range of $0.03 < \tau_j^* < 0.06$ were well represented, indicating that partial transport was dominant. Our fully mobile channels (Redwood and Grouse Creeks) had values of $\tau_j^*$ mostly greater than 0.06, indicating that, over most of the channel, all particles were mobilized in proportion to their abundance in bed material. Full mobility probably dominated bed load transport more than indicated by relative frequencies of $\tau_j^*$ alone, particularly in Jacoby Creek, because zones of full transport would likely correspond to zones of high transport rates. Fully mobile channels had high sediment supplies; partially mobile channels had low or moderate sediment supplies.

Relative areas of full mobility as predicted by our calculations of $\tau_j^*$ compared favorably with the extent of bed mobility, which was measured as scour and fill of cross sections. In water year 1998, peak discharge (650 m$^3$ s$^{-1}$) in Redwood Creek at the gaging station at Orick downstream of Redwood 1 was approximately bank-full. In Redwood 1 we estimated that 60% of the bed area was fully mobile at bank-full stage; surveys of cross section 20 (in Redwood 1) during summers preceding

**Figure 4.** Fine patch in trough, Redwood Creek 1.

and following this peak flow season showed that 62% of the bed width underwent significant changes (>±5 cm) in local bed elevation. Similarly, 80% of the bed area in Redwood 2 was deemed fully mobile; 82% of cross section 5 and 52% of cross section 6 (in Redwood 2) showed significant change (V. Ozaki and M. A. Madej, unpublished data, Redwood National Park, Arcata, California, 1999). In comparison, we estimated that 19% of the bed area of the Jacoby Creek study reach was fully mobile at bank-full stage. Three cross sections surveyed there before and after a bank-full event of April 11, 1980 [*Lisle*, 1989], showed that an average of 28% of the bed width underwent significant changes in bed elevation.

### 5.3. Dimensionless Bed Load Transport Rate

Frequency distributions of local dimensionless bed load transport rates of the median subsurface particle size ($W^*_{s50}$) showed contrasting patterns between partially mobile and fully mobile channels (Figure 5c). A reference transport rate ($W^*_r = 0.002$ [*Parker and Klingeman*, 1982]) representing near-threshold conditions can be used to evaluate distributions of $W^*_{s50}$. Partially mobile channels had highly skewed distributions with low transport rates ($W^*_{s50} < W^*_r$) heavily represented, while fully mobile channels exhibited a strong second mode in the range $W^*_{s50} > 1$. Jacoby Creek showed an intermediate distribution, with a weaker mode at $W^*_{s50} = 0.5$ and a stronger mode at $W^*_{s50} < 0.002$. All channels exhibited significant areas of very weak sediment transport.

We used frequency distributions of $q_{s50}$ to evaluate proportions of total load transported by fractions of the bed area ($f_j$) ranked in order of local transport rate ($q_{s50j}$):

$$F_{qs50j} = f_j q_{s50j} / \Sigma_j (f_j q_{s50j}).$$

Small portions of these channels conveyed major portions of the bed material load. For example, 90% of the load was conveyed by 6–49% of the bed area (Table 3). This percentage was greater in the more mobile channels.

## 6. Reach Scale: Bed Mobility Parameters

We focus on two reach-averaged, bed mobility parameters computed for bank-full stage: Shields stress ($\bar{\tau}^*$) and an adaptation of $Q^*$ of *Dietrich et al*. [1989] (uppercase designating a reach-averaged value). Alternative methods were used to compute $\bar{\tau}^*$ and $Q^*$: a data-intensive method based on local values of transport parameters and another based on reach-mean hydraulic variables and particle sizes. The former requires a lengthy program of data collection and analysis as described in this study; the latter requires more conventional techniques that could be accomplished in a few days or less. We compare values computed from the two methods to determine if the second method provides a satisfactorily accurate evaluation of bed mobility.

### 6.1. Mean Shields Stress

We computed mean Shields stress using alternative methods:

$$\overline{\tau^*_j} = \sum \tau^*_j / n, \tag{3a}$$

where $n$ is the number of values of local $\tau^*_j$ measured over a rectangular grid and

$$\hat{\bar{\tau}}^* = \bar{\tau}_G / R\bar{D}_{50j}, \tag{3b}$$

where $\bar{\tau}_G = \rho g \bar{d} S_G$ is the component of total mean boundary shear stress that is exerted on bed particles, $\overline{D_{50j}}$ is mean surface $D_{50}$, $\bar{d}$ is mean depth, and $S_G$ is the energy slope attributed to grain resistance (computed according to *Parker and Peterson* [980]). The former mean ($\overline{\tau_j^*}$) quantifies average surface more accurately because it is computed from coupled values of $\tau_j$ and $D_{50j}$.

All channels barely met or exceeded threshold conditions based on mean $\tau^*$. That is, once fines were computationally stripped from highly mobile patches, values of $\overline{\tau_j^*}$ (0.025–0.096) fell within a characteristic range for gravel-bed channels with mobile pavements (Table 3). The channels with the highest sediment yields (Redwood 1 and 2 and Grouse) had values of $\overline{\tau_j^*}$ (0.075–0.096) that are well above conventional entrainment thresholds (0.03–0.06 [*Buffington and Montgomery*, 1997]) and above the threshold of full mobility [*Wilcock and McArdell*, 1997]. Values of $\overline{\tau_j^*}$ (0.025–0.031) for the remainder (Jacoby Creek, Gunnison River, and Williams Fork) were within the range of entrainment thresholds. However, despite low values of $\overline{\tau_j^*}$ in these channels, bed material could be mobilized in areas of locally high $\tau_j^*$ (Figure 5b).

The alternative value ($\hat{\bar{\tau}}^*$) was a poor predictor of $\overline{\tau_j^*}$ but did a fair job of distinguishing channels according to their bed mobility. Differences between $\overline{\tau_j^*}$ and $\hat{\bar{\tau}}^*$ in a channel were as great as 70% (Table 3). However, values of $\hat{\bar{\tau}}^*$ would consistently match the channels according to low (Williams Fork), moderate (Jacoby Creek), and high sediment yields (Redwood and Grouse Creeks).

### 6.2. $Q^*$

In adapting the method of *Dietrich et al.* [1989], we defined $Q^*$ as the ratio of the mean predicted transport rate of the reach-averaged median particle size of subsurface material ($\overline{D_{s50}}$) given the armoring measured by the surface particle size ($D_{50j}$) to the transport rate of $\overline{D_{s50}}$ assuming there is no armoring ($D_{50j} = \overline{D_{s50}}$):

$$Q^* = \frac{\overline{q_{s50}(\tau_j, D_{50j})}}{\overline{q_{s50}(\tau_j, \overline{D_{s50}})}}, \tag{4a}$$

where $q_{s50}$ is a function of the parameters in parentheses according to (2). We assumed that $\overline{D_{s50}}$ represents the median particle size of bed load everywhere. Because we did not compute $Q^*$ from predicted transport rates of the total bed load, our values are not directly comparable to those of *Kinerson* [1990] or *Lisle et al.* [1993]. Moreover, our $Q^*$ is a ratio of mean local transport rates.

The alternative method was to use reach-mean values of boundary shear stress and surface particle size to compute mean transport rates of $\overline{D_{s50}}$,

$$\hat{Q}^* = \frac{\hat{\bar{q}}_{s50}(\overline{\tau_G}, \overline{D_{50j}})}{\hat{\bar{q}}_{s50}(\bar{\tau}_G, \overline{D_{s50}})}, \tag{4b}$$

as done by *Kinerson* [1990] and *Lisle et al.* [1993] for the total load.

A third alternative would have been to evaluate the difference in particle size between $D_{50}$ predicted at assumed mean bank-full threshold boundary shear stress and $\overline{D_{50j}}$ [*Buffington and Montgomery*, 1999]. We chose not to do this because we anticipated that the wide range in mean particle size among the reaches would affect variations in this difference.

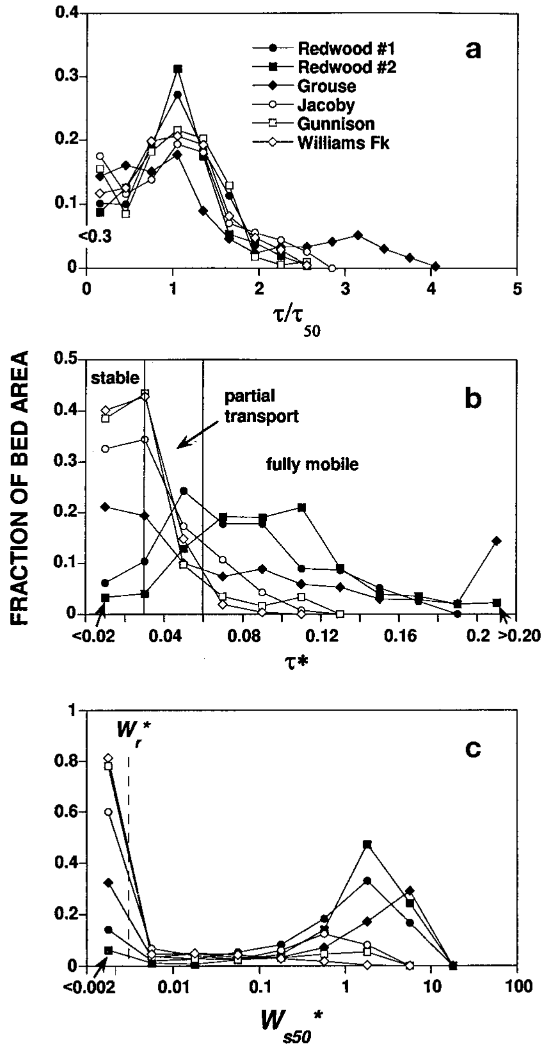


**Figure 5.** Frequency distributions of bed mobility parameters at bank-full stage: (a) local boundary shear stress normalized by median values for each reach, (b) local Shields stress, and (c) local dimensionless bed load transport rate. Fine sediment has been computationally stripped. Solid symbols indicate fully mobile channels; open symbols indicate partially mobile channels.

Values of $Q^*$ and $\hat{Q}^*$ (Table 3) varied with relative rates of sediment yield as predicted by the hypothesis of *Dietrich et al.* [1989]. Differences between $Q^*$ and $\hat{Q}^*$ in each channel were similar to those between $\overline{\tau_j^*}$ and $\hat{\bar{\tau}}^*$ except in those channels with low $Q^*$ (<0.1). Uncertainties in predicted mean transport rates and particle size distributions of the load, which are used to compute $Q^*$ and $\hat{Q}^*$, must be considered, however.

In the course of computing $Q^*$ and $\hat{Q}^*$, it became apparent that values of bed load transport computed from local values of particle size and boundary shear stress differed widely from those computed from reach-mean values. Mean bed load transport rate ($\hat{\bar{q}}_{s50}$) computed from mean $\tau^*$ (however the average is computed) tends to underpredict the mean of local transport rates ($\overline{q_{s50j}}$). This is because $q_{s50}$ (as well as transport rates for any size fraction) is a nonlinear function of $\tau^*$, which skews the distribution of $q_{s50j}$ toward high values rela-

**Table 3.** Bed Load Transport Parameters

| | $r$ for $\tau_j = f[(D_{50})]$[a] | Percent of Area Transporting 90% of Load | $\bar{\tau}_j^*$ | $\bar{\hat{\tau}}^*$ | $Q^*$[b] | $\hat{Q}^*$ |
|---|---|---|---|---|---|---|
| Redwood 1 | 0.27/0.41[c] | 39[b] | 0.11/0.075[c] | 0.13 | 0.36 | 0.59 |
| Redwood 2 | −0.36/−0.35 | 49 | 0.22/0.094 | 0.12 | 0.42 | 0.65 |
| Grouse Creek | 0.25/0.27 | 24 | 0.15/0.096 | 0.12 | 0.52 | 0.39 |
| Jacoby Creek | 0.19/0.18 | 20 | 0.040/0.033 | 0.060 | 0.13 | 0.12 |
| Gunnison River | 0.22 | 8 | 0.029 | NC[d] | 0.09 | NC[d] |
| Williams Fork | −0.30 | 6 | 0.025 | 0.019 | 0.03 | 0.07 |

[a]Correlation coefficient for boundary shear stress versus median surface particle size.
[b]Values are computationally stripped of fine material.
[c]Values to the left of the slash are for original bed material; those to the right are computationally stripped of fine material.
[d]NC indicates short reach length prevented calculation of a precise value.

tive to the distribution of $\tau_j^*$. We examined this discrepancy by evaluating the ratio $\hat{q}_{s50}/\overline{q_{s50j}}$ for each channel. Values of $\hat{q}_{s50}/\overline{q_{s50j}}$ were very low ($10^{-2}$) for values of $\overline{\tau_j^*} \leq 0.03$ and approached 1 (agreement) at values of $\overline{\tau_j^*} \geq 0.07$ (Figure 6). This resulted because bed load transport rates starting with the weakest rates near the entrainment threshold (e.g., $\tau^* \simeq 0.03$) initially increase rapidly with increasing $\tau^*$ and then increase less rapidly as general transport occurs (e.g., $\tau^* > 0.06$) [*Parker*, 1990; *Andrews and Smith*, 1992]. Thus at low transport stages the distribution of $q_{s50j}$ was highly skewed, and bed load transport was highly concentrated spatially. Bed load transport predictions based on mean hydraulic variables can be expected to be very inaccurate on a percentage basis, although inaccuracies at these low transport rates may not significantly affect values of total sediment flux computed for a wide range of flow.

A high degree of armoring may not be associated with low sediment supply and vice versa, because high boundary shear stress in excess of the entrainment threshold of the bed surface is the controlling factor of bed mobility [*Dietrich et al.*, 1989; *Buffington and Montgomery*, 1999]. For example, Williams Fork, which had a low sediment supply, was weakly armored ($\overline{D_{50j}}/\overline{D_{s50}} = 1.2$) but had low values of $Q^*$ and $\overline{\tau_j^*}$; Grouse Creek, which had a high sediment supply, was strongly armored ($\overline{D_{50j}}/\overline{D_{s50}} = 3.0$) but had high values of $Q^*$ and $\overline{\tau_j^*}$ (Table 3). Relations between $Q^*$, $\tau^*$, and armoring are shown in Figure 7. Contours of armoring were calculated by multiplying the terms within parentheses in the denominator of (4b) by $D_{s50}/D_{50}$ and solving for $Q^*$ for each value of $\tau^*$. For any degree of armoring, transport rates and thus $Q^*$ must approach zero as values of $\tau^*$ approach the entrainment threshold of the bed surface.

Finally, armoring should be measured by the relative particle sizes of the bed surface and the load, which can be overestimated by the subsurface size [*Leopold*, 1992; *Lisle*, 1995]. Thus there is uncertainty in values of $Q^*$ for these channels, with the exception of Redwood and Jacoby Creeks where particle size distributions of bed load were measured and shown to be nearly equal to those of subsurface bed material [*Lisle*, 1995].

## 7. Discussion and Conclusions

### 7.1. Local Scale: Balance Between Local Boundary Shear Stress and Bed Material Size

The apparent coexistence of zones of high bed mobility and immobility in the same channel is similar to the observations of *Lisle et al.* [1993] in an experimental channel. In this experi-

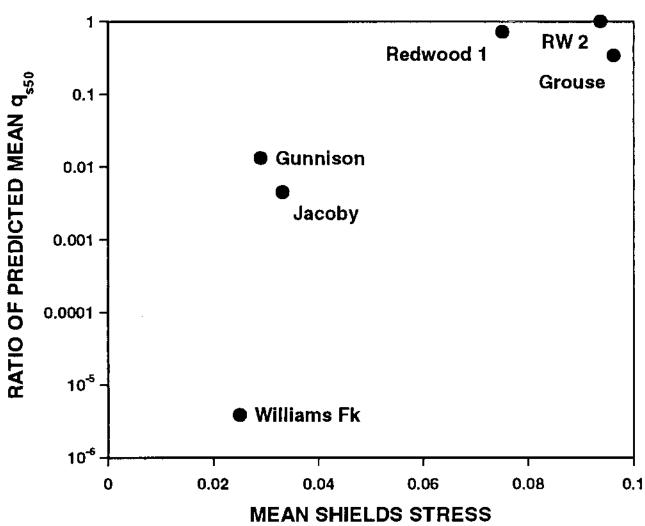


**Figure 6.** Ratio of mean bed load transport rate computed from mean boundary shear stress and bed-surface particle size to the mean of predicted local bed load transport rates versus mean Shields stress at bank-full stage.

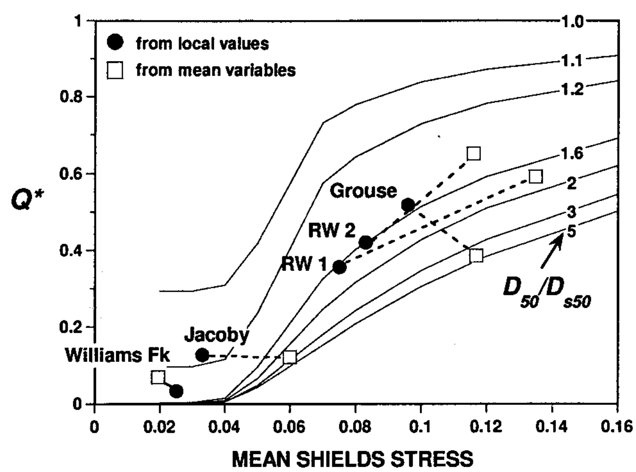


**Figure 7.** Variation of $Q^*$ with mean Shields stress computed from equations (3a) and (4a) (circles) and (3b) and (4b) (squares). Contours show variation of $Q^*$ with Shields stress for equal values of the degree of armoring ($D_{50}/D_{s50}$).

ment, alternate bars were allowed to form in a gravel-sand mixture, and changes in bed texture were measured as the rate of feeding the same mixture into the flume was decreased in two steps. As the channel first achieved equilibrium under the high feed rate, bed load transport was trained by bar morphology into a continuous lane bordered by immobile bed material. When feed rate was reduced, the bed surface coarsened, and the lane of bed load transport contracted. This coarsening reduced bed mobility, as mean boundary shear stress acting on surface particles remained nearly constant. A similar trend was evident in comparisons of the six natural channels reported here. The relative area of full mobility was greatest in the channels with high sediment supply, but even in these there were significant areas of immobility. We could not detect an effect of sediment supply on the distribution of boundary shear stress; all channels exhibited similar distributions of normalized shear stress.

Different channel types (meandering, braided, and alternate bar) show various adjustments between local boundary shear stress and surface particle size. Channel curvature and bed topography in alluvial meanders with heterogeneous bed material force strong spatial variations in boundary shear stress, sediment transport, and bed material size [*Dietrich and Smith*, 1984; *Parker and Andrews*, 1986]. Divergence of local boundary shear stress and bed topography are balanced by cross-stream sediment transport and surface particle size, creating lanes of high bed load transport [*Dietrich and Smith*, 1984; *Dietrich and Whiting*, 1989]. Equilibrium can be maintained by balancing local shear stress, bed material size, and transport rates, but imbalances commonly cause stage-dependent scour and fill of the bed, particularly in pools [*Andrews*, 1979; *Sear*, 1996]. Such adjustments are similar in straight or sinuous channels with alternate bars [*Andrews and Nelson*, 1989; *Whiting and Dietrich*, 1991], but divergence in boundary shear stress that promotes sorting may not be as strong as in meanders. In active braided channels, discontinuities in bed load transport in chute-and-pool systems drive episodic evolution at the reach scale [*Ashmore and Parker*, 1983; *Ashworth and Ferguson*, 1986; *Ferguson et al*., 1992]. Lack of a threshold adjustment between local shear stress and particle size creates rapidly evolving areas of intense bed load transport, as well as inactive areas [*Davoren and Mosley*, 1986; *Ashworth et al*., 1992]. Strong discontinuities in bed load transport in braided channels indicate that they depart from threshold adjustments more so than do single-thread channels with alternate bars or meanders.

Our purpose was not to revisit mechanisms of sorting and transport of sediment over channels with bar-pool topography but to evaluate the degree of adjustment between boundary shear stress and surface particle size and examine the effect of sediment supply. *Whiting and Dietrich* [1991] argue that the low exceedance of critical boundary shear stress on a bar in a straight reach of a gravel-bed channel with a moderate sediment supply limits departures from the threshold relation between surface particle size and boundary shear stress. Our data show that shear stress and particle size were poorly correlated at bank-full stage and that threshold conditions were not widely met. Boundary shear stress was locally much less than critical, indicating that much of the bed was inactive at bank-full stage. In other areas, particularly in channels with a high sediment supply, local boundary shear stress greatly exceeded critical shear stress. If such areas were very fine-grained, they might generate only moderate transport rates, but our calculations confirmed that bed load transport rates were, indeed, locally high. High supplies of sediment broadened active areas of the channel but did not apparently improve relations between shear stress and particle size because of the creation of extremely mobile zones. We hypothesize that the lack of correlation was partly caused by stage-dependent adjustments of surface particle size to the changing shear stress field. We measured surface particle size at low flow but modeled boundary shear stress for bank-full flow. However, computationally stripping fine material from fine areas with high Shields stress did not substantially improve the correlation between shear stress and particle size, and it is unlikely that coarse areas with low shear stress would become substantially finer during high flow.

Distributions of normalized values of boundary shear stress were roughly similar among the channels (Figure 5a). This indicates that the alternate-bar topography shared by all of the channels produced similar distributions of boundary shear stress.

Poor correlation between boundary shear stress and surface particle size has important ecological implications. Shields stress can represent the ability of benthic organisms to safely occupy a site, because it relates the local hydraulic environment (e.g., near-bed velocity and turbulent fluctuations) to dimensions of benthic microhabitat that are controlled by particle size (e.g., substrate interstices and wake zones). At very low $\tau_j^*$ (<0.01) the substrate is stable, and benthic organisms would not likely be displaced. At higher $\tau_j^*$ and particularly when the bed becomes at least partially mobile ($\tau_j^* > 0.03$), benthic organisms would more likely be displaced by high bottom velocities or mobilization of bed particles. The wide range in values of Shields stress that we observed in relatively simple gravel-bed channels indicates a tendency toward complexity in the association between benthic substrates and hydraulic conditions. Frequency distributions of $\tau_j^*$ (Figure 5b) suggest that at bank-full flow, high-velocity sites with mobile substrates are somewhat limited and that low-velocity sites with coarse, stable substrates provide enough refuges to maintain populations of organisms adapted to stable substrates. "Safe" sites ($\tau_j^* < 0.01$) were about twice as abundant (approximately 40% of bed area) in "partially mobile" channels with low sediment supply than in "fully mobile" channels with high sediment supply (≤20% of bed area). "Hazardous" sites ($\tau_j^* > 0.06$) comprised <20% of partially mobile channels and >50% of fully mobile channels.

We conclude that uniform threshold conditions are not characteristic of natural gravel-bed channels with alternate bars, as well as meandering or braided channels. Instead, local imbalances appear to drive stage-dependent scour and fill (degree 3 of adjustment, see section 1) and channel evolution (degree 4). This suggests the following conceptual model for channel evolution. As a channel evolves, mobile areas of the channel with high boundary shear stress and relatively fine bed material are prone to rapid morphologic change as they convey the bulk of the bed load. At the same time, areas with low boundary shear stress and coarse material that were created during earlier stages of channel evolution remain inactive. Nevertheless, they help create the boundary conditions to steer the flow and drive sediment transport in more mobile areas of the channel. At subsequent stages in evolution, active areas may become inactive and vice versa.

### 7.2. Reach Scale: Effects of Sediment Load on Bed Mobility

Detailed measurements of bed texture and hydraulic variables were used to compute reach-averaged mobility parameters in six natural channels having wide differences in sediment supply. An apparent relation between bed mobility and sediment supply supports the hypothesis of *Dietrich et al*. [1989], previously supported mainly by experimental results, that heterogeneous gravel beds adjust surface particle size to offer more or less resistance to transport in response to variations in sediment supply.

However, contrasts in sediment supply were also associated with contrasts in flow frequency, which may have affected differences in bed texture similarly. Competent flows in the channels with the highest sediment supply (Redwood and Grouse Creeks) are produced by rainfall, while competent flows in the channels with the lowest sediment supply (Gunnison River and Williams Fork) are usually produced by snowmelt. Comparisons of flow frequencies in these two regions show that runoff is most variable in California rivers [*Pitlick*, 1994], which, in particular, lack the long recessional hydrographs typical of nival floods. If intensive bed load transport produced more mobile bed-surface conditions during floods, such textures would be preserved best in California rivers where the duration of moderate flows that are capable of selectively transporting fine bed material and winnowing the armor layer is less. This suggests that fine particles should be more abundant on channel surfaces in California, regardless of sediment supply. The effect of flow frequency on bed textures deserves further research.

Another complicating factor is the abundance of fine sediment in bed material. Grouse and Redwood Creeks, which are highly mobile channels with high sediment loads, have large proportions of sand, which could also increase mobility by reducing surface roughness [*Iseya and Ikeda*, 1987]. It would be difficult to sort out the relative effects of a high rate of supply of bed load material and an enrichment of the channel with fine material that commonly accompanies accelerated erosion.

We tested alternative averaging techniques for computing reach-mean mobility parameters (bank-full Shields stress and $Q^*$) in order to identify a diagnostic parameter that would be useful for watershed managers. For each parameter a more practicable version was computed from mean hydraulic variables and bed material particle sizes, and a more accurate but costly version was computed from the mean of local values of the parameter. Reasonable agreement was achieved between alternative versions for both parameters, insofar as qualitative differences in sediment load would be correctly distinguished. Therefore the more practicable versions for evaluating bed mobility show promise for watershed managers, but their uncertainty suggests that they should be used as first-order assessments and interpreted in context with sediment budgeting. Using $\tau^*$ to evaluate bed mobility has advantages over $Q^*$ in avoiding the uncertainty of the particle size of the sediment load. A useful value of mean $\tau^*$ for some management applications can be obtained from careful measurements of reach-averaged variables, including hydraulic radius, channel gradient, bed-surface particle size, and discharge. (Mean velocity is obtained from discharge measurements and used to compute the boundary shear stress exerted on bed particles.) Field measurements do not require sampling of subsurface bed material nor otherwise estimating the particle size of the load. The primary advantage of $Q^*$ is that transport rates embodied in this parameter can be linked directly to imposed changes in load from the watershed; thus $Q^*$ may have greater capability than Shields stress in predicting channel response. Though it is doubtful that these methods can detect any less than a doubling of reach-scale increases in sediment supply, we argue that evaluations of bed mobility can be less uncertain than directly evaluating variations of supply from the watershed, which is usually confounded by uncertainties in delivery and routing of sediment through drainage networks. If the simpler versions of mobility parameters are to be used, we recommend that results be related to estimations of changes in sediment input, transport, and storage in upstream reaches.

**Acknowledgments.** Sue Hilton supervised data collection and performed much of the data analysis. Jack Lewis helped with preliminary runs of the flow model. Alice Berg, Scott Bowman, Carrie Jones, Meredith Manning, Chris Shivelle, Sherry Skillwoman, Stephen Stringall, and Yvonne Woodward assisted in data collection for the California channels. We are grateful to all for their vital help in this investigation. Reviews by John Buffington, Trevor Hoey, and Peter Wilcock greatly improved the paper.

## References

Andrews, E. D., Scour and fill in a stream channel, East Fork River, western Wyoming, *U.S. Geol. Surv. Prof. Pap*., *1117*, 49 pp., 1979.

Andrews, E. D., Entrainment of gravel from naturally sorted riverbed material, *Geol. Soc. Am. Bull*., *94*, 1225–1231, 1983.

Andrews, E. D., and D. C. Erman, Persistence in the size distribution of surficial bed material during an extreme snowmelt flood, *Water Resour. Res*., *22*(2), 191–197, 1986.

Andrews, E. D., and J. M. Nankervis, Effective discharge and the design of channel maintenance flows for gravel-bed rivers, in *Natural and Anthropogenic Influences in Fluvial Geomorphology*: *The Wolman Volume*, *Geophys. Monogr. Ser*., vol. 89, edited by J. E. Costa et al., pp. 151–164, AGU, Washington, D. C., 1995.

Andrews, E. D., and J. M. Nelson, Topographic response of a bar in the Green River, Utah, to variation in discharge, in *River Meandering*, *Water Resour. Monogr*., vol. 12, edited by S. Ikeda and G. Parker, pp. 463–485, AGU, Washington, D. C., 1989.

Andrews, E. D., and J. D. Smith, A theoretical model for calculating marginal bedload transport rates of gravel, in *Dynamics of Gravel-Bed Rivers*, edited by P. Billi et al., pp. 41–54, John Wiley, New York, 1992.

Antonia, R. A., and R. E. Luxton, The response of a turbulent boundary layer to a step change in surface roughness, Part 1, Smooth-to-rough, *J. Fluid Mech*., *48*, 721–762, 1971.

Antonia, R. A., and R. E. Luxton, The response of a turbulent boundary layer to a step change in surface roughness, Part 2, Rough-to-smooth, *J. Fluid Mech*., *53*, 737–758, 1972.

Ashmore, P., and G. Parker, Confluence scour in coarse braided streams, *Water Resour. Res*., *19*(2), 392–402, 1983.

Ashworth, P. J., and R. I. Ferguson, Interrelationships of channel processes, changes and sediments in a proglacial braided river, *Geogr. Ann*., *68A*, 361–371, 1986.

Ashworth, P. J., and R. I. Ferguson, Size selective entrainment of bed load in gravel bed streams, *Water Resour. Res*., *25*, 627–634, 1989.

Ashworth, P. J., R. I. Ferguson, and M. D. Powell, Bedload transport and sorting in braided channels, in *Dynamics of Gravel-Bed Rivers*, edited by P. Billi et al., pp. 497–515, John Wiley, New York, 1992.

Barkett, B. L., The relationship between grain size and shear stress in two gravel bed streams, M.S. thesis, Univ. of Colo., Boulder, 1998.

Buffington, J. M., and D. R. Montgomery, A systematic analysis of eight decades of incipient motion studies, with special reference to gravel-bedded rivers, *Water Resour. Res*., *33*(8), 1993–2029, 1997.

Buffington, J. M., and D. R. Montgomery, Effects of sediment supply on surface textures of gravel-bed rivers, *Water Resour. Res*., *35*(11), 3523–3530, 1999.

Davoren, A., and M. P. Mosley, Observations of bedload movement, bar development and sediment supply in the braided Ohau River, *Earth Surf. Processes Landforms*, *11*, 643–652, 1986.

Dietrich, W. E., and J. D. Smith, Bed load transport in a river meander, *Water Resour. Res*., *20*(10), 1355–1380, 1984.

Dietrich, W. E., and P. J. Whiting, Boundary shear stress and sediment transport in river meanders of sand and gravel, in *River Meandering*, *Water Resour. Monogr*., vol. 12, edited by S. Ikeda and G. Parker, pp. 1–50, AGU, Washington, D. C., 1989.

Dietrich, W. E., J. W. Kirchner, H. Ikeda, and F. Iseya, Sediment

supply and the development of the coarse surface layer in gravel-bedded rivers, *Nature*, *340*, 215–217, 1989.
Ferguson, R. I., K. L. Pretegaard, and P. J. Ashworth, Influence of sand on hydraulics and gravel transport in a braided gravel bed river, *Water Resour. Res*., *25*, 635–643, 1989.
Ferguson, R. I., P. J. Ashmore, P. J. Ashworth, C. Paola, and K. L. Prestegaard, Measurements in a braided river chute and lobe, 1, Flow pattern, sediment transport, and channel change, *Water Resour. Res*., *28*(7), 1877–1886, 1992.
Iseya, F., and H. Ikeda, Pulsations in bedload transport rates induced by a longitudinal sediment sorting: A flume study using sand and gravel mixtures, *Geogr. Ann*., *69A*, 15–27, 1987.
Keller, E. A., Areal sorting of bed-load material: The hypothesis of velocity reversal, *Geol. Soc. Am. Bull*., *82*, 753–756, 1971.
Kinerson, D., Surface response to sediment supply, M.S. thesis, Univ. of Calif., Berkeley, 1990.
Lane, E. W., Design of stable channels, *Trans. Am. Soc. Civ. Eng*., *120*, 1234–1279, 1955.
Lehre, A. K., and G. Carver, Thrust faulting and earthflows: Speculations on the sediment budget of a tectonically active drainage basin, in *American Geomorphological Field Group 1985 Field Trip Guidebook*, edited by H. M. Kelsey, T. E. Lisle, and M. E. Savina, pp. 169–183, Humboldt State Univ., Arcata, Calif., 1985.
Leopold, L. B., Sediment size that determines channel morphology, in *Dynamics of Gravel-Bed Rivers*, edited by P. Billi et al., pp. 297–311, John Wiley, New York, 1992.
Lisle, T. E., Stabilization of a gravel channel by large streamside obstructions and bedrock bends, Jacoby Creek, northwestern California, *Geol. Soc. Am. Bull*., *97*, 999–1011, 1986.
Lisle, T. E., Sediment transport and resulting deposition in spawning gravels, north coastal California, *Water Resour. Res*., *25*(6), 1303–1319, 1989.
Lisle, T. E., Particle size variations between bed load and bed material in natural gravel bed channels, *Water Resour. Res*., *31*(4), 1107–1118, 1995.
Lisle, T. E., and S. Hilton, Fine bed material in pools of natural gravel-bed channels, *Water Resour. Res*., *35*(4), 1291–1304, 1999.
Lisle, T. E., and M. A. Madej, Spatial variation in armouring in a channel with high sediment supply, in *Dynamics of Gravel-Bed Rivers*, edited by P. Billi et al., pp. 277–296, John Wiley, New York, 1992.
Lisle, T. E., F. Iseya, and H. Ikeda, Response of a channel with alternate bars to a decrease in supply of mixed-size bedload: A flume experiment, *Water Resour. Res*., *29*(11), 3623–3629, 1993.
Nelson, J. M., and J. D. Smith, Flow in meandering channels with natural topography, in *River Meandering*, *Water Resour. Monogr*., vol. 12, edited by S. Ikeda and G. Parker, pp. 69–102, AGU, Washington, D. C., 1989.
Parker, G., Hydraulic geometry of active gravel rivers, *J. Hydraul. Div. Am. Soc. Civ. Eng*., *105*(HY9), 1185–1201, 1979.
Parker, G., Surface-based bedload transport relation for gravel rivers, *J. Hydraul. Res*., *28*(4), 417–436, 1990.
Parker, G., and E. D. Andrews, On the time devolpment of meander bends, *J. Fluid Mech*., *162*, 139–156, 1986.
Parker, G., and P. C. Klingeman, On why gravel bed streams are paved, *Water Resour. Res*., *18*(5), 1409–1423, 1982.
Parker, G., and A. W. Peterson, Bar resistance of gravel-bed streams, *J. Hydraul. Div. Am. Soc. Civ. Eng*., *106*(HY10), 1559–1575, 1980.
Patankar, S. V., *Numerical Heat Transfer and Fluid Flow*, McGraw-Hill, New York, 1980.
Pitlick, J., Relation between peak flows, precipitation, and physiography for five mountainous regions in the western USA, *J. Hydrol*., *158*, 219–240, 1994.
Raines, M. A., and H. M. Kelsey, Sediment budget for the Grouse Creek basin, Humboldt County, California, final report, 110 pp., Six Rivers Natl. For., Eureka, Calif., 1991.
Rattray, M., and E. Mitsuda, Theoretical analysis of conditions in a salt wedge, *Estuarine Coastal Mar. Sci*., *2*, 373–394, 1974.
Sear, D. A., Sediment transport processes in pool-riffle sequences, *Earth Surf. Processes Landforms*, *21*, 241–262, 1996.
Simon, A., and C. R. Thorne, Channel adjustment of an unstable coarse-grained stream: Opposing trends of boundary and critical shear stress, and the applicability of extremal hypotheses, *Earth Surf. Processes Landforms*, *21*, 155–180, 1996.
Van Steeter, M. M., and J. Pitlick, Geomorphology and endangered fish habitats of the upper Colorado River, 1, Historic changes in streamflow, sediment load and channel morphology, *Water Resour. Res*., *34*(2), 287–302, 1998.
Whiting, P. J., and W. E. Dietrich, Convective accelerations and boundary shear stress over a channel bar, *Water Resour. Res*., *27*(5), 783–796, 1991.
Wilcock, P. R., and B. W. McArdell, Partial transport of a sand/gravel sediment, *Water Resour. Res*., *33*(1), 235–245, 1997.
Wilcock, P. R., and J. B. Southard, Bed-load transport of mixed-size sediment: Fractional transport rates, bed forms, and the development of a coarse bed-surface layer, *Water Resour. Res*., *25*(7), 1629–1641, 1989.
Wolman, M. G., A method of sampling coarse river bed material, *Eos Trans. AGU*, *35*(6), 951–956, 1954.

B. L. Barkett and J. Pitlick, Department of Geography, University of Colorado, Boulder, CO 80309. (pitlick@spot.colorado.edu)
T. E. Lisle, Pacific Southwest Research Station, U.S. Forest Service, Arcata, CA 95521. (tel7001@axe.humboldt.edu)
M. A. Madej, U.S. Geological Survey, Arcata, CA 95521. (mary_ann_majed@usgs.gov)
J. M. Nelson, U.S. Geological Survey, Denver, CO 80225-0046. (jmn@usgs.gov)

(Received January 31, 2000; revised August 3, 2000;
accepted August 4, 2000.)